Original Article

Osseointegration and fixation opportunities of sacroiliac instrumentation: a preclinical evaluation in a large animal model

David W. Polly Jr[1,2], Michael J. Gardner[3], Dan Wills[4], James Crowley[4], Matthew Pelletier[4], Tian Wang[4], Ian Bailey[5], Scott Yerby[5], William R. Walsh[4]

[1]Department of Orthopaedic Surgery, University of Minnesota, Minneapolis, MN, USA; [2]Department of Neurosurgery, University of Minnesota, Minneapolis, MN, USA; [3]Department of Orthopaedic Surgery, Stanford University School of Medicine, Stanford, CA, USA; [4]Surgical and Orthopaedic Research Laboratories, Prince of Wales Clinical School, University of New South Wales, Sydney, AUS; [5]SI-BONE, Inc., Santa Clara, CA, USA

Contributions: (I) Conception and design: DW Polly, MJ Gardner, WR Walsh, S Yerby; (II) Administrative support: I Bailey, S Yerby; (III) Provision of study materials or patients: WR Walsh, S Yerby; (IV) Collection and assembly of data: WR Walsh, D Wills, J Crowley, M Pelletier, T Wang; (V) Data analysis and interpretation: D Wills, J Crowley, M Pelletier, T Wang, I Bailey, S Yerby; (VI) Manuscript writing: All authors; (VII) Final approval of manuscript: All authors.

Correspondence to: David W. Polly Jr, MD. Department of Orthopaedic Surgery, University of Minnesota, 2450 Riverside Avenue South, Suite R200, Minneapolis, MN 55454, USA; Department of Neurosurgery, University of Minnesota, Minneapolis, MN, USA. Email: pollydw@umn.edu.

Background: Implant fixation is often the cornerstone of musculoskeletal surgical procedures performed to provide bony fixation and/or fusion. The aim of this study was to evaluate how different design features and manufacturing methods influence implant osseointegration and mechanical properties associated with fixation in a standardized model in cancellous bone of adult sheep.

Methods: We evaluated the *in vivo* performance of three titanium alloy implants: (A) iFuse-TORQ implant; (B) Fenestrated Sacroiliac Device; and (C) Standard Cancellous Bone Screw in the cancellous bone of the distal femur and proximal tibia in 8 sheep. Group A was produced using additive manufacturing [three-dimensional (3D) printing] while Groups B and C were made with traditional methods. The *vivo* responses of the implants at the implant-bone interface were examined using mechanical testing (push out and removal torque), polymethyl methacrylate (PMMA) histology combined with fluorochrome labels and quantitative histomorphometry of bone ongrowth, ingrowth and through growth at 3 and 6 weeks.

Results: New bone formed directly on all groups and no adverse reactions were noted. Osseointegration via ongrowth, ingrowth and through growth was a function of implant design. Implant designs that provide osseointegration via ongrowth, ingrowth and through growth improve implant fixation in torsion. The 3D printed surface in group A was rougher and outperformed traditional manufacturing surfaces of groups B and C in torsion. The porous domains and fenestrations in the design of group A allowed for bone ingrowth and through growth, which accounted for the superior torsional properties.

Conclusions: Implant designs that provide osseointegration via ongrowth, ingrowth and through growth improve implant fixation.

Keywords: Bony fixation; pelvic implants; osseointegration; bioingrowth screw; SI joint

Submitted Jun 04, 2024. Accepted for publication Aug 29, 2024. Published online Nov 11, 2024.
doi: 10.21037/jss-24-67
View this article at: https://dx.doi.org/10.21037/jss-24-67

Introduction

Implant fixation is often the cornerstone of musculoskeletal surgical procedures performed to provide bony fixation and/or fusion. Osseointegration, first defined by Albrektsson and co-workers (1,2) as "direct contact (at the light microscope level) between living bone and implant" plays a vital role in implant fixation. In cases where an implant directly interfaces with bone, the load magnitude, complexity, and frequency sometimes overcome the interface strength and subsequent loosening or device failure may result (3). Iliosacral screw fixation has become commonplace for unstable posterior pelvic ring fractures as well as chronic sacroiliac joint (SIJ) pain (3-5). Internal screw fixation, while effective, can lead to screw backout or failure with the repetitive cyclic motion across an unfused joint.

The concept of a bioingrowth screw that accomplishes fixation and fusion through osseointegration is attractive for fixation. Osseointegration opportunities at the bone-implant interface can be achieved via new bone formation directly on the surface of an implant (ongrowth), new bone formation within the porous domains of an implant (bone ingrowth), new bone formation through an implant (through growth) as well as combinations of all three. These concepts have been quantified as early as the 1980's through analysis of retrieved porous implants (6-12). Strategies to improve the opportunities of biological fixation have been the topic of many preclinical studies evaluating materials, surface treatments, coatings, topography, porosity, and surgical site as well as preparation (13-32). Additive manufacturing has allowed implant designers to incorporate a number of bony incorporation features such as surface texture, porosity, and fenestrations that can provide pathways for osseointegration at the implant-bone interface (33-36) and potentially improved long-term clinical outcomes through a stable implant-bone interface.

The current study was designed to better understand the bony interactions of commonly used pelvic implants in a standardized ovine cancellous implantation model in healthy skeletally mature animals. The implants included an additively manufactured implant with pores and large fenestrations, an anodized implant with large fenestrations, and a standard bone screw; all implants were titanium alloy (Ti64). We hypothesized that the additively manufactured implant would have greater biologic fixation and torque-out relative to the other two implants based on implant topography and geometry. We present this article in accordance with the ARRIVE reporting checklist (available at https://jss.amegroups.com/article/view/10.21037/jss-24-67/rc).

Highlight box

Key findings

- Longer-term implant stability may reduce or prevent screw backout in pelvic trauma patients. It may also improve fusion rates in patients treated for sacroiliac joint disorders, as has been observed with a 3D printed triangular implant with similar features.

What is known and what is new?

- In cases where an implant directly interfaces with bone, the load magnitude, complexity, and frequency sometimes overcome the interface strength and subsequent loosening or device failure may result.
- The concept of a bioingrowth screw that accomplishes fixation and fusion through osseointegration is attractive for fixation.

What is the implication, and what should change now?

- The implants evaluated in the current study highlight the opportunities of osseointegration that can be achieved through three mechanisms: bone ongrowth, ingrowth, and through-growth.
- Future preclinical work where these implants are evaluated across a joint or fracture and longer time point would be warranted as well as evaluation of these implants in humans.

Methods

Three titanium alloy implants were evaluated: Group A: 11.5 mm × 40 mm diameter threaded implant with porous lattice surface, helical bone harvesting flutes, and fenestrations (iFuse-TORQ, SI-BONE, Santa Clara, CA, USA); Group B: 12 mm × 40 mm smooth screw with fenestrations (RIALTO, Medtronic, Minneapolis, MN, USA); and Group C: 7.3 mm × 40 mm trauma screw with smooth surface (SI-BONE, Santa Clara, CA, USA). Group A was produced using additive manufacturing (3D printing) while Groups B and C were manufactured with traditional subtractive methods. Experiments were performed under project license (20/162A) granted by the Animal Care and Ethics Committee, Division of Research, Research Ethics and Compliance Support Unit, in compliance with University of New South Wales institutional guidelines for the care and use of animals. No protocol (including the research question, key design features, and analysis plan) was prepared before the study.

Statistical analysis

The maximum pushout force, energy to failure and ultimate

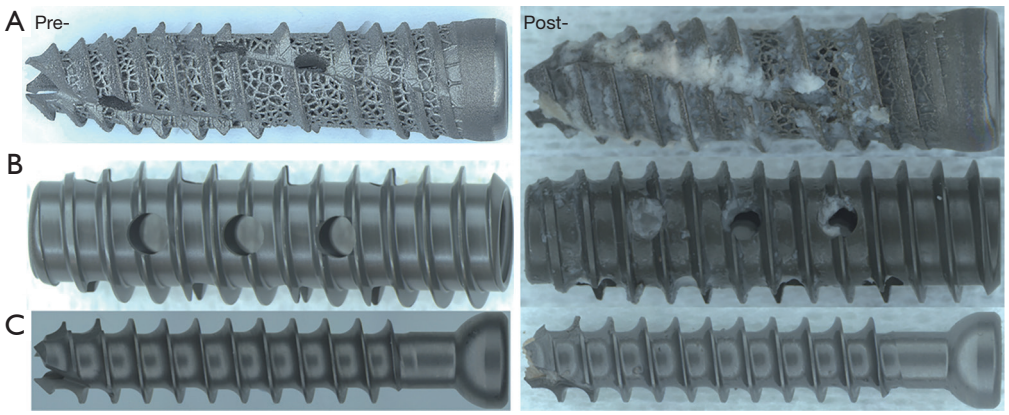

Figure 1 Images of Group A–C implants pre- and post-implantation at time zero. Note the autograft material present in the pores and fenestrations of the Group A implant and in the fenestrations of the Group B implant. Group A: 11.5 mm × 40 mm diameter threaded implant with porous lattice surface, helical bone harvesting flutes, and fenestrations (iFuse-TORQ, SI-BONE, Santa Clara, CA, USA), Group B: 12 mm × 40 mm smooth screw with fenestrations (RIALTO, Medtronic, Minneapolis, MN, USA), and Group C: 7.3 mm × 40 mm trauma screw with smooth surface (SI-BONE, Santa Clara, CA, USA).

shear strength, torque versus time was analyzed using a two-way analysis of variance (ANOVA) and Tukey honestly significant difference (HSD) post-hoc test. The ANOVA followed by a Games Howell post hoc test was performed on the histomorphometry data using International Business Machines (IBM) Statistical Package for the Social Sciences (SPSS) (Version 27) for all statistical analyses.

Time zero evaluations

One implant from each Group was evaluated using stereozoom microscopy (Leica M125 C, Leica North Ryde, Australia) to inspect the implant surface features (*Figure 1*). Time zero surgery (n=2 of each implant design) was performed to assess the surgical preparation and tapping procedures (outlined below) for any self-grafting of local bone based on the designs. The amount of bone captured by implant during insertion was determined by weighing the implants before and after insertion into cancellous bone using a calibrated laboratory balance.

In vivo evaluations

Eight healthy skeletally mature cross-bred wethers (sheep) were enrolled in this study following institutional ethical clearance (Approval 20/162A); these animals are independent of those described in the t=0 testing. Twenty-four hours prior to surgery, pre-emptive analgesia was administered, by applying a transdermal fentanyl patch (100 mg – 2 mcg/kg/hr) to the right foreleg of each animal. Implantation sites in the cancellous bone of medial distal femurs and proximal tibiae were prepared using combinations of drilling and tapping using fluoroscopic guidance for trajectory (*Figure 2* and *Table 1*). Implantation sites were randomized on the day of surgery. Sample size was considered based on torsional testing with an effect size of 2 with alpha at 0.05 and power 0.8 using G*Power software.

Implants in Group A were inserted by placing a 3.2-mm guide pin followed 7.5 and 8.5 mm cannulated drills. A 10.75-mm cannulated tap was used prior to implantation. Implants in Group B were inserted by placing a 2.0-mm guide pin followed by an 8.5 mm drill and 12 mm tap. Implants in Group C were inserted by placing a 2.0-mm guide pin followed by a 5-mm drill and tap. All drilling procedures were irrigated with room temperature saline during drilling. Animals were housed in deep litter in standard floor pens throughout the study. Animals were monitored throughout the project by dedicated staff for signs of pain or any adverse reactions.

Animals in the 6-week group were given bone labels at 3 weeks (Engemycin®, 20 mg/kg, IM) and the day prior to euthanization (Calcein Green, 10 mg/kg, IM). Animals were euthanized at 3- and 6-week following surgery. The harvested hind limbs were radiographed in the anteroposterior and lateral planes using a Faxitron and digital plates (Agfa CR MD4.0 Cassette). An Agfa Digital Developer and workstation were used to process the digital

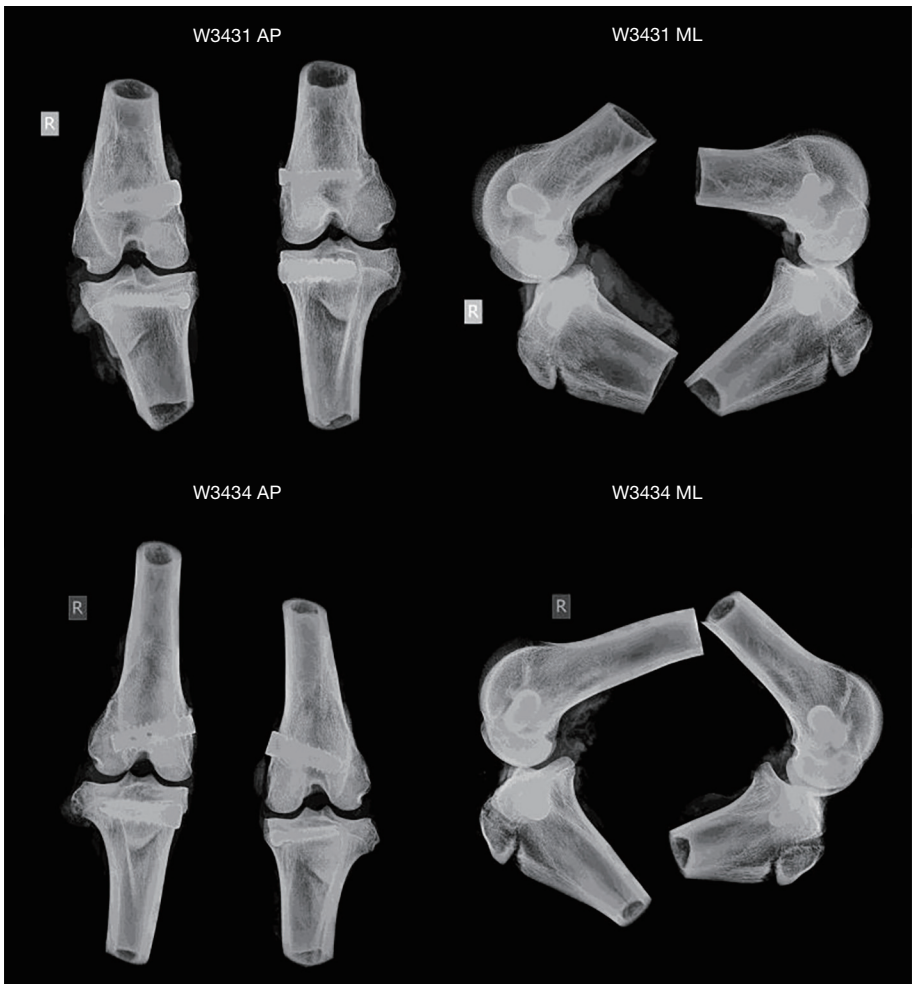

Figure 2 Implants placed in the left and right distal femurs and proximal tibiae of each animal. The location of each implant was systematically varied between animals to reduce anatomical site biases. AP, anterior posterior; ML, mediolateral.

Table 1 Treatment groups

Group	Name	Material	Diameter (mm)	Length (mm)	Manufacturer
A	iFuse TORQ	Add Mfg Ti 64 Alloy	11.5	40	SI-BONE, Santa Clara, CA, USA
B	RIALTO	Anodized Ti 64 Alloy	12.0	40	Medtronic, Minneapolis, MN, USA
C	Generic bone screw (investigational design)	Ti 64 Alloy	7.3	40	SI-BONE, Santa Clara, CA, USA

Group A: 11.5 mm × 40 mm diameter threaded implant with porous lattice surface, helical bone harvesting flutes, and fenestrations (iFuse-TORQ, SI-BONE, Santa Clara, CA, USA); Group B: 12 mm × 40 mm smooth screw with fenestrations (RIALTO, Medtronic, Minneapolis, MN, USA); and Group C: 7.3 mm × 40 mm trauma screw with smooth surface (SI-BONE, Santa Clara, CA, USA). TORQ, SI-BONE iFUSE TORQ implant.

images (Agfa CR 75.0 Digitiser Musica, Agfa, Germany). The Digital Imaging and Communications in Medicine (DICOM) data were converted to Joint Photographic Experts Group (JPEG) images using ezDICOM medical viewer. The Faxitron radiographs were evaluated for evidence of adverse reactions in a blinded fashion. The

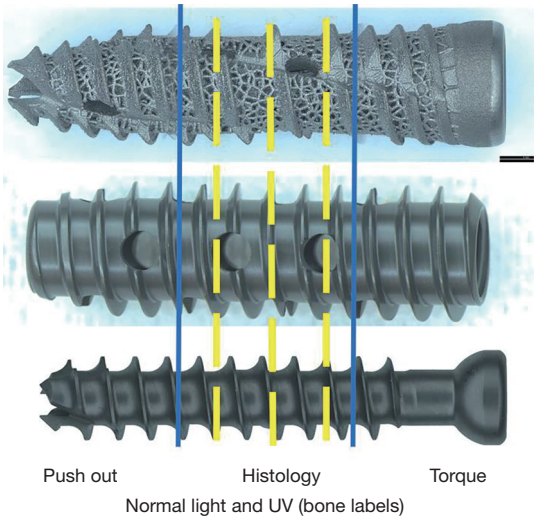

Figure 3 Implant regions designated for push out (distal), histology (mid-section) and torque out (proximal) for each implant. The yellow dashed lines represent where the histology sections were taken. UV, ultraviolet.

implants and surrounding cancellous bone were prepared to allow perpendicular sections (*Figure 3*) to provide a push out sample for the distal portion, a histological sample for the mid-portion and finally a sample for torsional testing from the proximal end. Mechanical testing was performed on the day of harvest and blinded to treatment group. Histology was reviewed blinded to time point.

Push out testing

The 15 mm sample from the distal portion was pushed out of the cancellous bone at 5 mm/min using a calibrated servohydraulic testing machine (MTS 858 Bionix, MTS System Corporation, Eden Prairie, MN, USA). The samples were supported with a rigid base and a hole slightly larger than each screw diameter. The implants were pushed into the hole without contacting the base to create a shear failure.

The shear stress was calculated according to Eq. [1].

$$\sigma = \frac{Load}{\left(\frac{C1+C2}{2}\right).\pi.d_i} \quad [1]$$

Eq. [1]: Shear stress calculation where c = bony thickness measurement from each side of the implant based on the histological slides (mm), di = diameter of the implant (mm).

Torsional testing

A 10-mm sample from the proximal portion was tested in torsion using a calibrated torque wrench and data acquisition (Transducer Techniques SWS-20, SSI, Temecula, CA, USA), to measure the removal torque. Each specimen was secured in a vice and the torque monitored while the torque wrench was rotated manually until failure.

PMMA histology

The portion of the samples allocated for histology were dehydrated through a series of increasing concentrations of ethanol, infiltrated with methylmethacrylate, and polymerized. A Leica SP1600 saw-microtome (Leica Microsystems Pty Ltd., North Ryde, Australia) was used to cut 3 sections (15–20 microns thick) perpendicular to the implant long axis (*Figure 3*). The sections were etched with acidic ethanol (98 mL ethanol 96% and 2 mL HCl 37%), stained with methylene blue followed by Basic Fuchsin (31). Stained sections were examined under light microscopy using an Olympus Microscope with an Olympus DP72 high resolution video camera (Olympus, Macquarie Park, Australia). Histology was qualitatively assessed at 3- and 6-week for general tissue responses, the presence of inflammatory cells or necrosis blinded by time at the bone-implant interface. Two additional unstained sections were cut in the 6-week group for analysis under ultraviolet (UV) light to assess any dynamic bone formation using the bone label injections. The bone-implant interface was examined for presence of the bone labels for each Group at 6 weeks.

Histomorphometry

Histomorphometry was performed on the images from the PMMA slides to determine the area percentage of the implant, bone tissue (new bone and marrow), and other soft tissues present in sections using a validated SORL custom program (32). Three slides at low magnification images (1.25×) were analyzed to determine bone ingrowth into porous regions (Group A) and bone ongrowth (Groups A–C) and through growth in the implant fenestrations (Group A and B). Ingrowth was measured as bone in the available void (BIAV). The materials or bone tissue (mineralized bone and bone marrow elements) was identified by pixel color and morphology and the area of each determined as

Table 2 Mechanical testing (mean ± standard deviation)

Group	Max pushout force (N)		Pushout stiffness (N/mm)		Max torque (Nm)		Shear stress (N/mm^2)	
	3 weeks	6 weeks	3 weeks	6 weeks	3 weeks	6 weeks	3 weeks	6 weeks
A	1,442±667	1,877±415	3,215±2,273	3,981±915	4.06±1.38*	11.64±4.16*	3.03±1.34	4.11±0.71
B	2,335±507	2,302±425	5,279±1,789	4,572±1,672	1.28±0.42	1.71±0.97*	4.32±0.46	4.62±1.17
C	1,249±273	2,005±103	3,653±564	4,767±603	0.33±0.23*	0.49±0.29*	4.03±1.06	6.82±0.55

Values with common superscripts (*) are significantly different (P<0.05). Group A: 11.5 mm × 40 mm diameter threaded implant with porous lattice surface, helical bone harvesting flutes, and fenestrations (iFuse-TORQ, SI-BONE, Santa Clara, CA, USA); Group B: 12 mm × 40 mm smooth screw with fenestrations (RIALTO, Medtronic, Minneapolis, MN, USA); and Group C: 7.3 mm × 40 mm trauma screw with smooth surface (SI-BONE, Santa Clara, CA, USA).

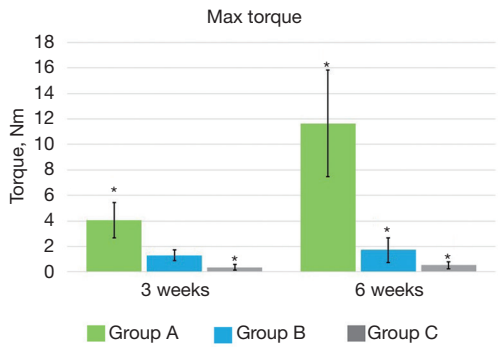

Figure 4 A bar chart of the average removal torque values. Bars with common superscripts (*) are significantly different (P<0.05). There error bars represent ± one standard deviation. Group A: 11.5 mm × 40 mm diameter threaded implant with porous lattice surface, helical bone harvesting flutes, and fenestrations (iFuse-TORQ, SI-BONE, Santa Clara, CA, USA); Group B: 12 mm × 40 mm smooth screw with fenestrations (RIALTO, Medtronic, Minneapolis, MN, USA); and Group C: 7.3 mm × 40 mm trauma screw with smooth surface (SI-BONE, Santa Clara, CA, USA).

a percentage of the regions of interest (ROI). A mean value was obtained for each animal based on the PMMA slides.

Results

Stereozoom images of implants before and after implanting and removing from cancellous bone at time zero (*Figure 1*) demonstrate the different osseointegration and fixation opportunities for each implant. The threads in the additive manufactured implant, Group A, were rougher compared to traditional machined implants (Groups B and C), which captured the host bone into the profile as well as increasing the overall surface area for bone ongrowth. Fenestrations are present in Groups A and B as well as the addition of porous substrate in Group A, which also had some bone present. The implant weights before and after inserting into cancellous bone were used to quantify how much bone is grafted into the implants revealed Group A to harvest 0.84±0.05 g, Group B 0.32±0.05 g and Group C 0.18±0.123 g.

The surgery was completed without any adverse events. All animals recovered uneventfully following surgery and were fully ambulating following recovery from anaesthesia and throughout the study period. There were no infections or adverse findings noted at harvest or any adverse bony reactions based on radiographs.

Mechanical testing of the distal portion of the implant in a push-out orientation did not reveal any significant difference for pushout force, pushout stiffness, or shear stress between the Groups at either 3 or 6 weeks (*Table 2*). The two-way ANOVA revealed group as well as time were significant as well as an interactive effective with group and time for torsional testing (P<0.05). Removal torque on the proximal portion of the implants revealed a significant improved between 3 and 6 weeks for Group A while no improvement was observed with time for Groups B and C. Removal torque for Group A outperformed Groups B and C at both time points (*Figure 4*).

PMMA histology at 3- and 6-week demonstrated osseointegration with the different features across the three implants evaluated. Direct bone ongrowth was found for the rough titanium surface in Group A as well as the machined surfaces present in Groups B and C (*Figure 5*). Bone ingrowth into the porous regions of implants in Group A was observed at 3 weeks with newly formed woven bone present within the implant that remodeled with time at 6 weeks. The cancellous graft material present because of the self-harvesting nature of Group A was also found within the porous regions participating in the new bone formation and remodeling at the implant-bone interface (*Figure 5*). New woven bone

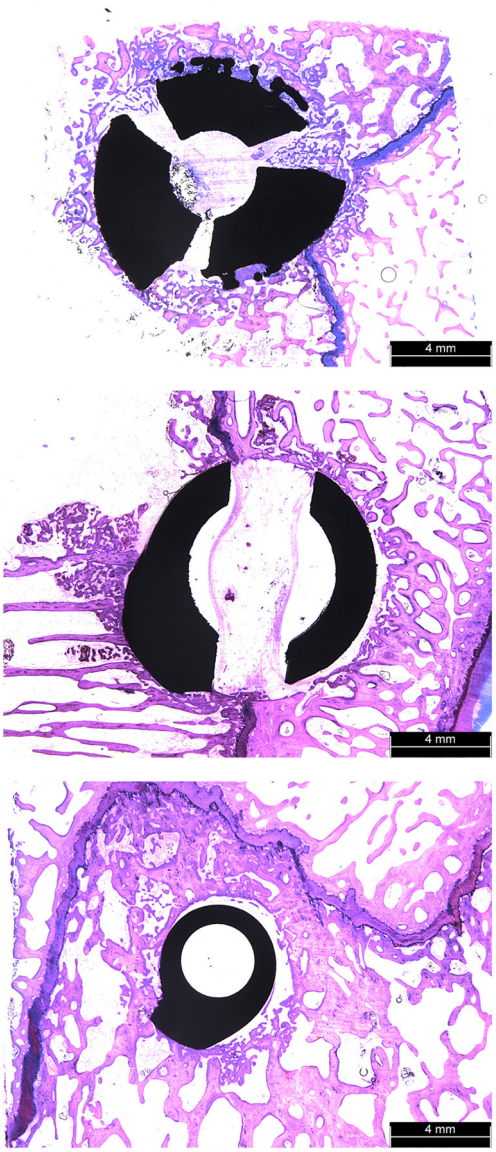

Figure 5 Examples of implant fixation and osseointegration opportunities. PMMA histology stained with methylene blue-basic fuchsin. The scale bar is present for the magnification. Group A (top) allows for ongrowth on the implant surface, ingrowth within the implant's porous surface, and through-growth within the implant's fenestrations. Group B (middle) allows for ongrowth and through-growth, and Group C (bottom) allows for ongrowth. Group A: 11.5 mm × 40 mm diameter threaded implant with porous lattice surface, helical bone harvesting flutes, and fenestrations (iFuse-TORQ, SI-BONE, Santa Clara, CA, USA); Group B: 12 mm × 40 mm smooth screw with fenestrations (RIALTO, Medtronic, Minneapolis, MN, USA); and Group C: 7.3 mm × 40 mm trauma screw with smooth surface (SI-BONE, Santa Clara, CA, USA). PMMA, polymethyl methacrylate.

formation was found within the fenestrations in Groups A and B that also remodeled with time (*Figure 5*).

Histomorphometry evaluated bone ongrowth, bone ingrowth, and bone through-growth at 3 and 6 weeks. There was no significant difference between the ongrowth and through-growth values between the Groups at either 3 or 6 weeks (*Table 3*, *Figure 6*). Only Group A implants were capable of ingrowth and were, therefore, not compared to other Group averages.

UV bone histology confirmed the actively healing bone interfaces for all implant Groups with time. Both labels were present in areas of bone ongrowth for all Groups as well as the ingrowth porous regions of Group A and the fenestrated areas filling with new bone (*Figure 7*).

Discussion

Implant fixation is a vital component of all devices implanted in bone for orthopaedic procedures including total joints (hips/knees/shoulders/ankles), spinal fusions, and dental applications. Strategies and technology to achieve implant fixation have evolved with a better understanding of biology/biomechanics/material science/engineering as well as clinical considerations depending on surgical implantation and *in vivo* loading requirements. Clinically, the implants used in this study would be placed across the SIJ for pelvic trauma or SIJ fixation. A controlled preclinical model was chosen with implants placed into the cancellous bone of the distal femur and proximal tibia of adult sheep bilaterally to provide a reproducible model of cancellous bone to evaluate osseointegration of different implants (24). Similar studies using the cancellous bone of the distal femur and proximal tibia have been useful in evaluating materials, manufacturing methods, geometry, coatings, and surface treatments for implants ultimately designed for joint replacement as well as interbody fusion devices (15-17,20-22,25-32). Time points of 3- and 6-week were chosen to focus on the *in vivo* responses in the early post-operative period. The features provided by the implants play an important role in osseointegration and early stability.

Radiographs confirmed no adverse bony reactions as well as placement but did not provide any other insight into osseointegration. Removal torque provided a sensitive means to evaluate implant fixation and Group A offered a significantly higher resistance to removal torque than the other two implants. This is likely attributed to bone ongrowth to the rougher titanium alloy surface of additive

Table 3 Histomorphometry (mean standard deviation)

Group	Ongrowth (mm)		Ingrowth (BIAV) (mm)		Through-growth (mm)	
	3 weeks	6 weeks	3 weeks	6 weeks	3 weeks	6 weeks
A	0.511±0.118	0.494±0.212	0.373±0.077	0.342±0.055	0.187±0.045	0.182±0.027
B	0.397±0.092	0.342±0.147	N/A	N/A	0.108±0.076	0.172±0.031
C	0.371±0.124	0.364±0.102	N/A	N/A	N/A	N/A

Group A: 11.5 mm × 40 mm diameter threaded implant with porous lattice surface, helical bone harvesting flutes, and fenestrations (iFuse-TORQ, SI-BONE, Santa Clara, CA, USA); Group B: 12 mm × 40 mm smooth screw with fenestrations (RIALTO, Medtronic, Minneapolis, MN, USA); and Group C: 7.3 mm × 40 mm trauma screw with smooth surface (SI-BONE, Santa Clara, CA, USA). BIAV, bone in the available void; N/A, not applicable.

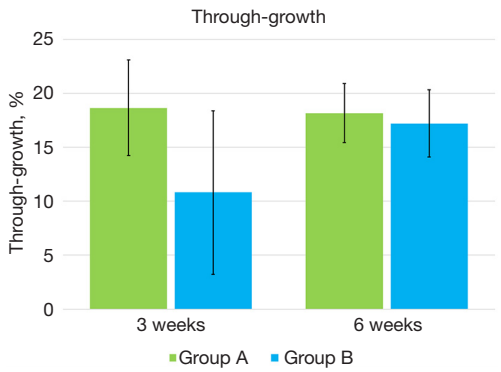

Figure 6 The ongrowth and through-growth for Groups A, B, and C. Only Groups A and B were capable of through-growth, therefore, Group C in not included in this comparison. Only Group A implants were capable of ingrowth and were, therefore, not compared to other Group averages. None of the comparisons are significantly different. Group A: 11.5 mm × 40 mm diameter threaded implant with porous lattice surface, helical bone harvesting flutes, and fenestrations (iFuse-TORQ, SI-BONE, Santa Clara, CA, USA); Group B: 12 mm × 40 mm smooth screw with fenestrations (RIALTO, Medtronic, Minneapolis, MN, USA); and Group C: 7.3 mm × 40 mm trauma screw with smooth surface (SI-BONE, Santa Clara, CA, USA).

manufacturing combined porous domains of the implant allowing for ingrowth compared to smoother titanium with no porous regions.

Histology at 3- and 6-week demonstrated that all implants offer some degree of ongrowth; this included the rougher titanium lattice surface in the additive manufacturing implants (Group A) as well as the smoother titanium surfaces in Groups B and C. The two implants with fenestrations also offered through-growth (Groups A and B) while only the Group A implants offered ingrowth via a porous surface. No adverse reactions in terms of inflammatory cells at the interface were noted to the titanium alloy of the additive manufactured implants of Group A or the subtractive manufacturing of Groups B and C. Surgical site preparation of drilling and tapping may also play a role in the *in vivo* response and potential long-term stability of the implant. Group A was noted to "harvest" host bone at the interface, which may enhance ingrowth due to the presence of autograft material that can participate in the healing response with time for ingrowth.

The implants evaluated in the current study highlight the opportunities of osseointegration that can be achieved through three mechanisms: bone ongrowth, ingrowth, and through-growth. Implant design determines how these osseointegration opportunities can be exploited to achieve implant stability in the short as well as longer term. Longer-term implant stability may reduce or prevent screw backout in pelvic trauma patients. It may also improve fusion rates in patients treated for SIJ disorders, as has been observed with a 3D printed triangular implant with similar features (23).

Our findings are concurrent with the work of MacBarb *et al.* (24) who used a similar ovine cancellous defect model to compare a machined solid triangular plasma sprayed implant with an additive manufactured fenestrated triangular implant with porous surfaces with and without hydroxyapatite coatings at 6 and 12 weeks. This study used a similar method of isolating different portions of the implant for biomechanics as well as histology. These authors reported excellent bone ongrowth, ingrowth, and through-growth while no differences were detected in mechanical testing using push-out modality between groups at each time point (24). The current study demonstrated that pushout testing of threaded implants is not very sensitive in distinguishing between implants that allow for varying degrees of biologic fixation. This is likely due the

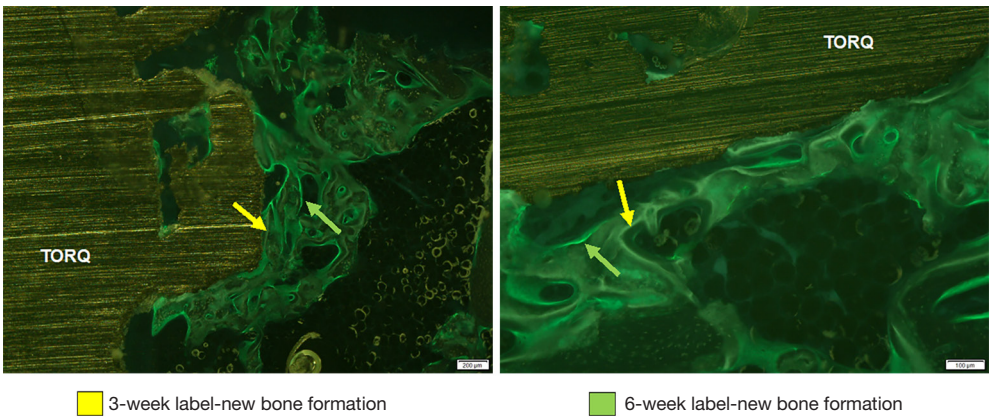

Figure 7 Two examples of new bone formation at 3 and 6 weeks indicated by arrows. PMMA histology stained with methylene blue-basic fuchsin. The scale bar is present for the magnification. The 3-week bone growth was identified using Engemycin and 6-week bone growth was identified using Calcein Green. TORQ, SI-BONE iFUSE TORQ implant; PMMA, polymethyl methacrylate.

interference of bone between the threads and resistance of this bone to shear during pullout as opposed to the shear bony failure at the implant interface experienced during torsion. This is relevant in pelvic fixation since screw backout is not uncommon while pullout is relatively uncommon.

The implants in Groups A and B are often used to treat degenerative and traumatic SIJ conditions via a lateral approach whereby the implant traverses though the ilium, across the SIJ, and terminates in the sacrum. The implants in Group A are also used in a sacro-alar iliac trajectory to supplement pelvic fixation implants in the setting of adult deformity surgery. The porous lattice on Group A increases the surface area available for osseointegration, allowing the implants the ability to provide stable fixation.

However, robust integration of bone to the implant may present challenges in case of implant revision or removal. Thin-walled trephines have been successfully used to free the implant from the host bone.

This study has limitations that need to be noted. The small sample size and short follow-up (6 weeks) precludes any comments on longer-term results. The animals used in this study were healthy and the cancellous sites used were not across any joint. Histology was also only performed on the middles section and thus proximal and distal implant design features were not examined. The gross implant geometries were different between Groups A–C. In addition, the subject implants are typically placed across a joint or a fracture, whereas the current study focused on the bone-implant interface and reaction in cancellous bone. Future preclinical work where these implants are evaluated across a joint or fracture and longer time point would be warranted as well as evaluation of these implants in humans.

Conclusions

Our study showed that implant designs that facilitate osseointegration via ongrowth, ingrowth and through growth improve implant fixation. The 3D printed surface in Group A was rougher, resulting in increased surface area for bone adherence, and outperformed the other groups in torsion. In addition, the porous domains, and fenestrations in the design of Group A allowed for bone ingrowth and through growth, which accounted for the superior mechanical properties in torsional testing. The large animal pre-clinical model used provides a useful means to evaluate different features present in screw designs.

Acknowledgments

This study was presented as a podium presentation at Orthopedic Research Society 2023 in Dallas, TX.
Funding: This study was funded by SI-BONE, Inc.

Footnote

Reporting Checklist: The authors have completed the ARRIVE reporting checklist. Available at https://jss.amegroups.com/article/view/10.21037/jss-24-67/rc

Data Sharing Statement: Available at https://jss.amegroups.com/article/view/10.21037/jss-24-67/dss

Peer Review File: Available at https://jss.amegroups.com/article/view/10.21037/jss-24-67/prf

Conflicts of Interest: All authors have completed the ICMJE uniform disclosure form (available at https://jss.amegroups.com/article/view/10.21037/jss-24-67/coif). M.P. serves as an unpaid editorial board member of *Journal of Spine Surgery* from May 2023 to April 2025. All authors report that this study was funded by SI-BONE. D.W.P. reports consultancies with SI-Bone, Globus, and Alexion, royalties SI Bone and Springer (textbook), research support from Medtronic and MizuhoOSI and Medtronic, and serves on the following professional organizations: Scoliosis Research Society, Minnesota Orthopaedic Society, North American Spine Society, and American Spine Registry. M.J.G. receives consulting fees and royalties from SI-BONE. D.W., M.P., T.W. and W.R.W. receive institutional research support from SIBONE. I.B., S.Y. are employed by SI-BONE and hold company stock options. The authors have no other conflicts of interest to declare.

Ethical Statement: The authors are accountable for all aspects of the work in ensuring that questions related to the accuracy or integrity of any part of the work are appropriately investigated and resolved. Experiments were performed under project license (20/162A) granted by the Animal Care and Ethics Committee, Division of Research, Research Ethics and Compliance Support Unit, in compliance with University of New South Wales institutional guidelines for the care and use of animals.

References

1. Albrektsson T, Albrektsson B. Osseointegration of bone implants. A review of an alternative mode of fixation. Acta Orthop Scand 1987;58:567-77.
2. Albrektsson T, Brånemark PI, Hansson HA, et al. Osseointegrated titanium implants. Requirements for ensuring a long-lasting, direct bone-to-implant anchorage in man. Acta Orthop Scand 1981;52:155-70.
3. Kebaish KM. Sacropelvic fixation: techniques and complications. Spine (Phila Pa 1976) 2010;35:2245-51.
4. Miller AN, Routt ML Jr. Variations in sacral morphology and implications for iliosacral screw fixation. J Am Acad Orthop Surg 2012;20:8-16.
5. Moshirfar A, Rand FF, Sponseller PD, et al. Pelvic fixation in spine surgery. Historical overview, indications, biomechanical relevance, and current techniques. J Bone Joint Surg Am 2005;87 Suppl 2:89-106.
6. Bloebaum RD, Mihalopoulus NL, Jensen JW, et al. Postmortem analysis of bone growth into porous-coated acetabular components. J Bone Joint Surg Am 1997;79:1013-22.
7. Cook SD, Barrack RL, Thomas KA, et al. Quantitative analysis of tissue growth into human porous total hip components. J Arthroplasty 1988;3:249-62.
8. Cook SD, Thomas KA, Haddad RJ Jr. Histologic analysis of retrieved human porous-coated total joint components. Clin Orthop Relat Res 1988;(234):90-101.
9. Marshall AD, Mokris JG, Reitman RD, et al. Cementless titanium tapered-wedge femoral stem: 10- to 15-year follow-up. J Arthroplasty 2004;19:546-52.
10. Schroeder A, van der Zypen E, Stich H, et al. The reactions of bone, connective tissue, and epithelium to endosteal implants with titanium-sprayed surfaces. J Maxillofac Surg 1981;9:15-25.
11. Bauer TW, Schils J. The pathology of total joint arthroplasty. I. Mechanisms of implant fixation. Skeletal Radiol 1999;28:423-32.
12. Spector M. Historical review of porous-coated implants. J Arthroplasty 1987;2:163-77.
13. Bandyopadhyay A, Espana F, Balla VK, et al. Influence of porosity on mechanical properties and in vivo response of Ti6Al4V implants. Acta Biomater 2010;6:1640-8.
14. Bandyopadhyay A, Mitra I, Shivaram A, et al. Direct comparison of additively manufactured porous titanium and tantalum implants towards in vivo osseointegration. Addit Manuf 2019;28:259-66.
15. Bertollo N, Da Assuncao R, Hancock NJ, et al. Influence of electron beam melting manufactured implants on ingrowth and shear strength in an ovine model. J Arthroplasty 2012;27:1429-36.
16. Bertollo N, Matsubara M, Shinoda T, et al. Effect of surgical fit on integration of cancellous bone and implant cortical bone shear strength for a porous titanium. J Arthroplasty 2011;26:1000-7.

17. Bertollo N, Sandrini E, Dalla Pria P, et al. Osseointegration of multiphase anodic spark deposition treated porous titanium implants in an ovine model. J Arthroplasty 2015;30:484-8.
18. Bobyn JD, Pilliar RM, Cameron HU, et al. The optimum pore size for the fixation of porous-surfaced metal implants by the ingrowth of bone. Clin Orthop Relat Res 1980;(150):263-70.
19. Bobyn JD, Stackpool GJ, Hacking SA, et al. Characteristics of bone ingrowth and interface mechanics of a new porous tantalum biomaterial. J Bone Joint Surg Br 1999;81:907-14.
20. Causey GC, Picha GJ, Price J, et al. In-Vivo response to a novel pillared surface morphology for osseointegration in an ovine model. J Mech Behav Biomed Mater 2021;119:104462.
21. Causey GC, Picha GJ, Price J, et al. The effect of a novel pillar surface morphology and material composition demonstrates uniform osseointegration. J Mech Behav Biomed Mater 2021;123:104775.
22. Chen D, Bertollo N, Lau A, et al. Osseointegration of porous titanium implants with and without electrochemically deposited DCPD coating in an ovine model. J Orthop Surg Res 2011;6:56.
23. Patel V, Kovalsky D, Meyer SC, et al. Prospective Trial of Sacroiliac Joint Fusion Using 3D-Printed Triangular Titanium Implants: 24-Month Follow-Up. Med Devices (Auckl) 2021;14:211-6.
24. MacBarb RF, Lindsey DP, Woods SA, et al. Fortifying the Bone-Implant Interface Part 2: An In Vivo Evaluation of 3D-Printed and TPS-Coated Triangular Implants. Int J Spine Surg 2017;11:16.
25. Svehla M, Morberg P, Bruce W, et al. No effect of a type I collagen gel coating in uncemented implant fixation. J Biomed Mater Res B Appl Biomater 2005;74:423-8.
26. Svehla M, Morberg P, Bruce W, et al. The effect of substrate roughness and hydroxyapatite coating thickness on implant shear strength. J Arthroplasty 2002;17:304-11.
27. Svehla M, Morberg P, Zicat B, et al. Morphometric and mechanical evaluation of titanium implant integration: comparison of five surface structures. J Biomed Mater Res 2000;51:15-22.
28. Walsh WR, Pelletier M, Wills D, et al. Undercut macrostructure topography on and within an interbody cage improves biomechanical stability and interbody fusion. Spine J 2020;20:1876-86.
29. Walsh WR, Pelletier MH, Bertollo N, et al. Does PEEK/HA Enhance Bone Formation Compared With PEEK in a Sheep Cervical Fusion Model? Clin Orthop Relat Res 2016;474:2364-72.
30. Walsh WR, Pelletier MH, Bertollo N, et al. Bone ongrowth and mechanical fixation of implants in cortical and cancellous bone. J Orthop Surg Res 2020;15:177.
31. Walsh WR, Pelletier MH, Christou C, et al. The in vivo response to a novel Ti coating compared with polyether ether ketone: evaluation of the periphery and inner surfaces of an implant. Spine J 2018;18:1231-40.
32. Walsh WR, Pelletier MH, Wang T, et al. Does implantation site influence bone ingrowth into 3D-printed porous implants? Spine J 2019;19:1885-98.
33. Agarwal R, Gupta V, Singh J. Additive manufacturing-based design approaches and challenges for orthopaedic bone screws: a state-of-the-art review. Journal of the Brazilian Society of Mechanical Sciences and Engineering 2022;44:37.
34. Burnard JL, Parr WCH, Choy WJ, et al. 3D-printed spine surgery implants: a systematic review of the efficacy and clinical safety profile of patient-specific and off-the-shelf devices. Eur Spine J 2020;29:1248-60.
35. McGregor M, Patel S, McLachlin S, et al. Data related to architectural bone parameters and the relationship to Ti lattice design for powder bed fusion additive manufacturing. Data Brief 2021;39:107633.
36. Wong KV, Hernandez A. A review of additive manufacturing. International Scholarly Research Notices 2012. Available online: https://doi.org/10.5402/2012/208760

Cite this article as: Polly DW Jr, Gardner MJ, Wills D, Crowley J, Pelletier M, Wang T, Bailey I, Yerby S, Walsh WR. Osseointegration and fixation opportunities of sacroiliac instrumentation: a preclinical evaluation in a large animal model. J Spine Surg 2024;10(4):616-626. doi: 10.21037/jss-24-67